Chapter 5

Empirical Characterization and VMD-Based Analysis of Speed Hump-Induced Vibrations

5.1 Preface

This chapter presents the comprehensive results and discussion of the experimental and analytical investigation of speed hump-induced vehicle vibrations. Building upon the signal acquisition and preprocessing pipeline detailed in Section 4.5, the chapter systematically examines multi-directional vibration responses (X, Y and Z directions) across a range of vehicle types and speed breaker profiles, namely Fiber, Bitumen and Rumble Strips.

The analysis includes unified time-frequency metrics (e.g., peak acceleration, RMS, energy, dominant frequency) and decomposition-based insights derived via Variational Mode Decomposition (VMD). Through these approaches, the study elucidates the influence of vehicle characteristics (mass, suspension, geometry) and speed breaker configurations (material stiffness, height/width ratio) on vibrational behavior. Results are structured to highlight how vibration responses vary across directional components and signal modes,

forming the basis for further discussions on vehicle-road dynamics and vibration mitigation strategies.

5.2 Results

This section presents the vibration responses of different vehicle types across Fiber, Bitumen and Rumble Strip profiles, systematically analyzed through multi-directional metrics (X, Y and Z axes). Variational Mode Decomposition (VMD) refines frequency-specific insights, capturing energy and modulation variations across intrinsic modes. Results reveal distinct vibration patterns influenced by hump geometry, vehicle type and directional orientation.

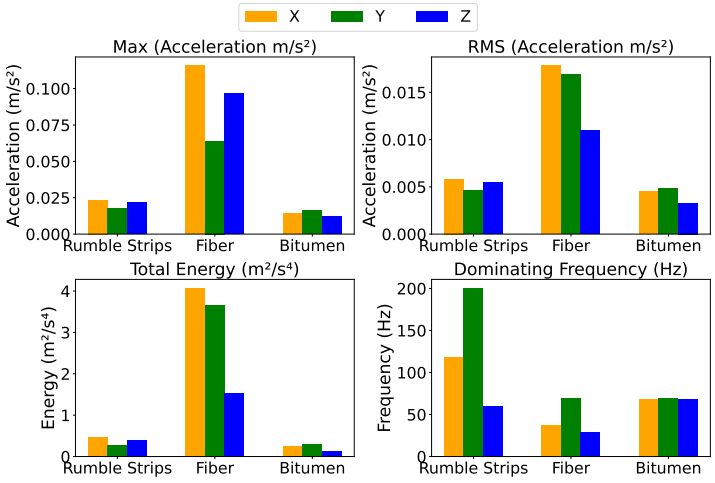

(a) LCV

Continued on next page

Figure 5.1 continued from previous page

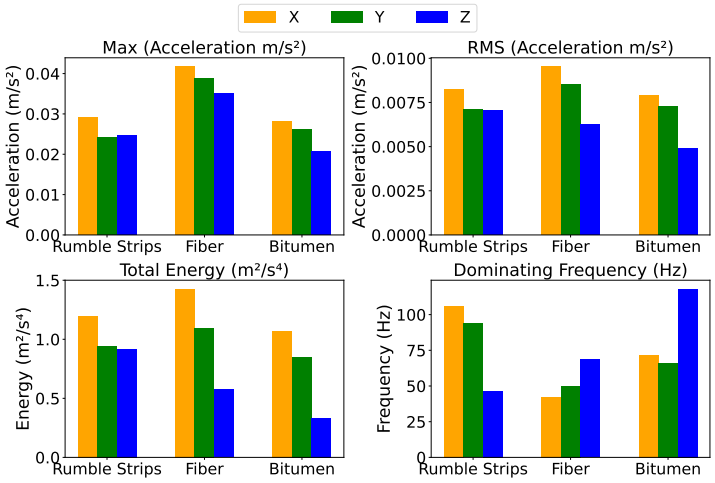

(b) Car

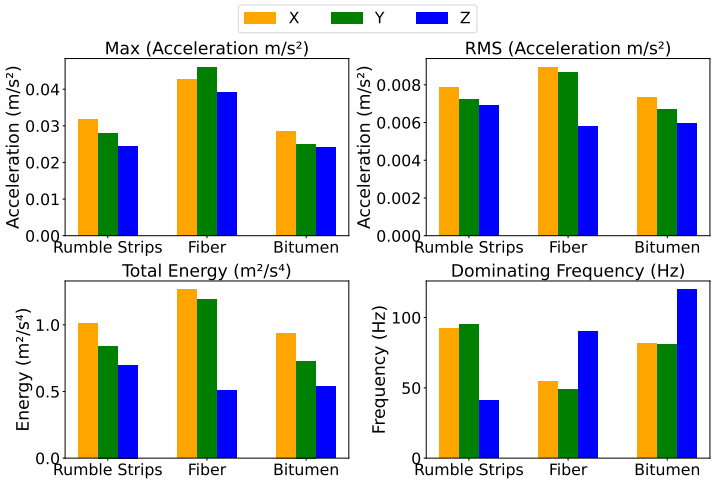

(c) 2-Wheeler

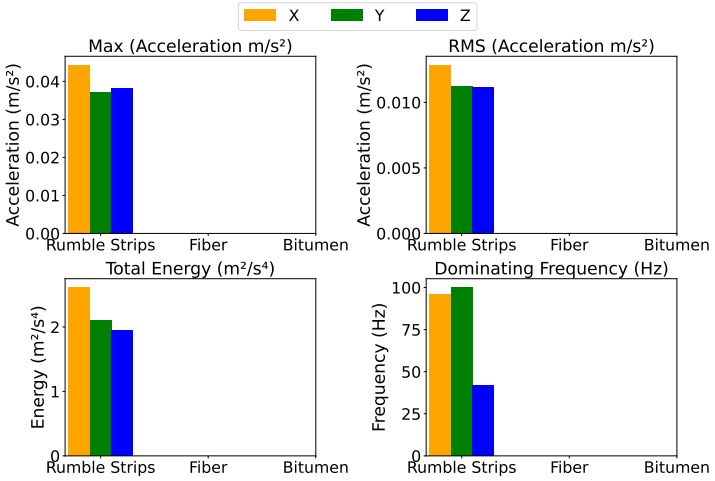

(d) Truck

Continued on next page

Figure 5.1 continued from previous page

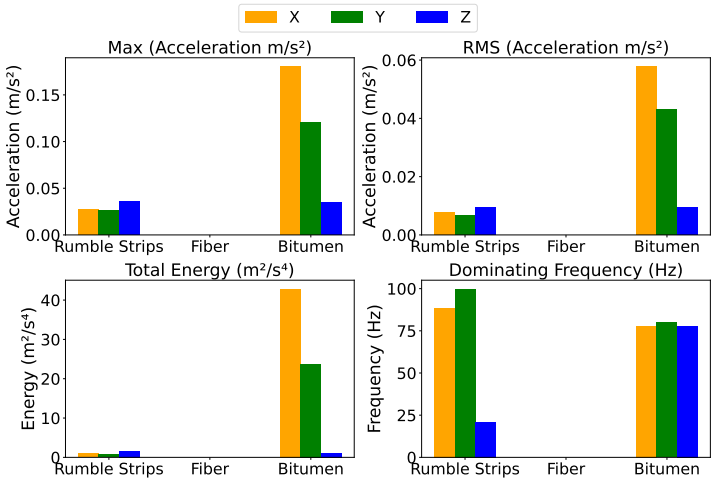

(e) Bus

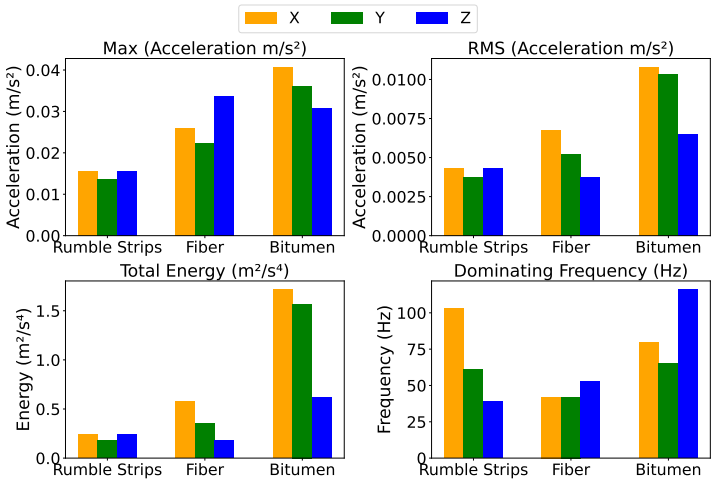

(f) 3-Wheeler

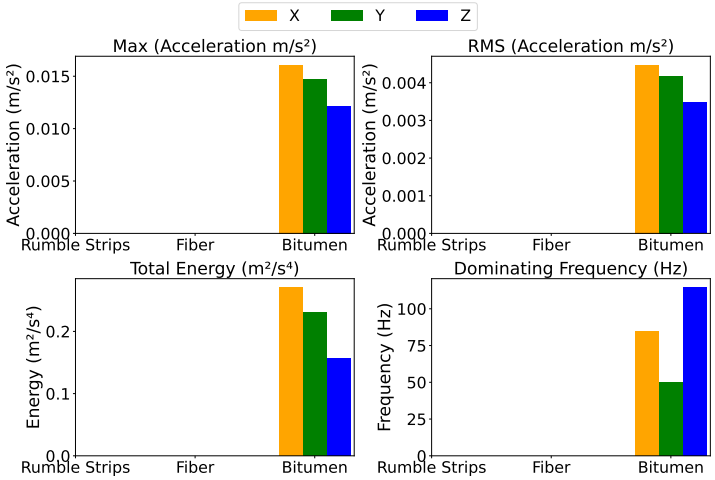

(g) 2-Wheeler Electric

Continued on next page

Figure 5.1 continued from previous page

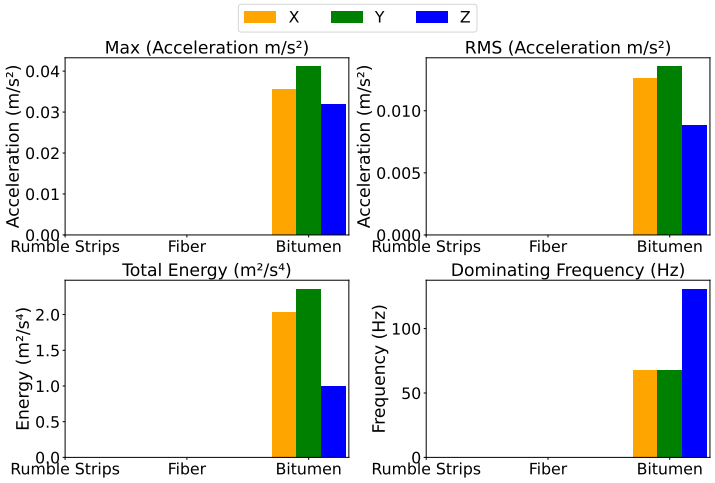

(h) E-Rickshaw

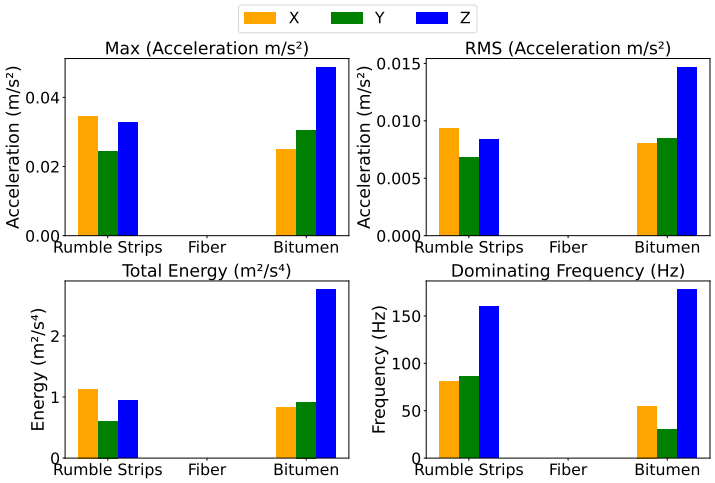

(i) Tractor

Fig. 5.1 Metrics for Different Vehicles Across Speed Breaker Types (X, Y, Z)

5.2.1 Unified Signal Vehicle Response Across Speed Breaker Types

The analysis of multi-directional vibrations generated by different vehicle types passing over various speed hump profiles (Fiber, Bitumen and Rumble Strips) was conducted using metrics including maximum acceleration, RMS acceleration, total energy and dominant frequency. These metrics were analyzed separately for the X, Y and Z directional components, as seen in Figure 5.1, where vehicle-wise matrices are presented. Each bar in the

plots represents the mean value of the respective metric computed across all trials for the corresponding vehicle-speed breaker combination.

Fiber Humps

For Fiber humps, the maximum acceleration in the X direction was highest for LCVs (0.1159 m/s^2) with a dominating frequency of 38 Hz, as shown in Figure 5.1. The 3-Wheeler exhibited the lowest value (0.026 m/s^2) with a frequency of 42 Hz. In the Y direction, LCVs also showed the highest value at 0.0639 m/s^2, while 3-Wheelers exhibited a lower maximum acceleration of 0.0223 m/s^2. In the Z direction, LCVs led again with 0.0966 m/s^2 at a frequency of 29 Hz, while the 3-Wheeler showed the lowest vertical acceleration of 0.0337 m/s^2. Total energy analysis revealed that the X direction for LCVs reached the highest energy at 4.078 m^2/s^4, whereas 3-Wheelers generated the least (0.578 m^2/s^4). Similar patterns were observed in the Y and Z directions, with LCVs demonstrating the highest total energy across all directions.

Bitumen Humps

For Bitumen humps, in the X direction, the highest maximum acceleration was recorded for the Bus (0.1807 m/s^2) at a dominant frequency of 78 Hz, while the lowest was for LCVs (0.0143 m/s^2). The Y direction showed the Bus with the highest value (0.1209 m/s^2), while 2-Wheelers Electric had a minimal acceleration of 0.0147 m/s^2, as shown in Figure 5.1. In the Z direction, the Bus also led with a maximum of 0.0345 m/s^2, while LCVs experienced the lowest vertical acceleration of 0.0122 m/s^2. Energy-wise, the X direction exhibited the highest total energy for the Bus (42.910 m^2/s^4) as depicted in Figure 5.1, whereas LCVs displayed the lowest energy at 0.263 m^2/s^4. This energy distribution trend was similarly reflected in the Y and Z directions, where the Bus consistently displayed substantial energy values across all directions.

Rumble Strips

For Rumble Strips, in the X direction, the Truck displayed the highest maximum acceleration (0.0444 m/s^2) with a dominating frequency of 95.76 Hz as shown in Figure 5.1, while the 3-Wheeler had the lowest value (0.016 m/s^2). In the Y direction, the Truck recorded a peak acceleration of 0.0372 m/s^2, whereas the 3-Wheeler exhibited a minimal value of 0.0137 m/s^2. In the Z direction, the Truck maintained its lead with a maximum acceleration of 0.0383 m/s^2. Total energy in the X direction was highest for Trucks (2.619 m^2/s^4) and lowest for 3-Wheeler (0.237 m^2/s^4). Consistent trends were observed in the Y and Z directions, where Trucks exhibited the highest energy values across all directional components.

5.2.2 Variational Mode Decomposition (VMD) for Multi-Modal Vehicle Vibration Analysis

This section presents the outcomes of applying Variational Mode Decomposition (VMD) to analyze multi-directional vibration signals collected from different vehicle types traversing various speed hump profiles. VMD effectively decomposed the signals into intrinsic mode functions, enabling the isolation of key vibration characteristics. In Figure 5.2, different modes are shown for the X direction signal of the truck passing over the rumble strip, like this other vehicle has different modes in all three directions. For each speed breaker type Fiber, Bitumen and Rumble Strips the extracted modes were evaluated based on metrics such as maximum amplitude, energy, dominant frequency, signal modulation, etc., across the X, Y and Z directions and shown only for the first two modes as in Tables 5.2, 5.3, 5.4 and 5.5 because modes beyond these are insignificant in maximum cases. In the tables, there are several abbreviations used to represent various VMD modes signal features: Mean (Mean), Var (Variance), Std Dev (Standard Deviation), RMS (Root Mean Square), Skew (Skewness), Kurt (Kurtosis), P-P (Peak-to-Peak), Max (Maximum), Min (Minimum),

Cr (Crest Factor), Ener (Energy), Sh E (Shannon Entropy), MME (Mean Modulation Energy), DF FFT (Dominant Frequency via FFT), DF PSD (Dominant Frequency via Power Spectral Density) and SNR (Signal-to-Noise Ratio). The following subsections provide a detailed, speed-breaker-wise analysis of the observed vibration characteristics and modal behaviors.

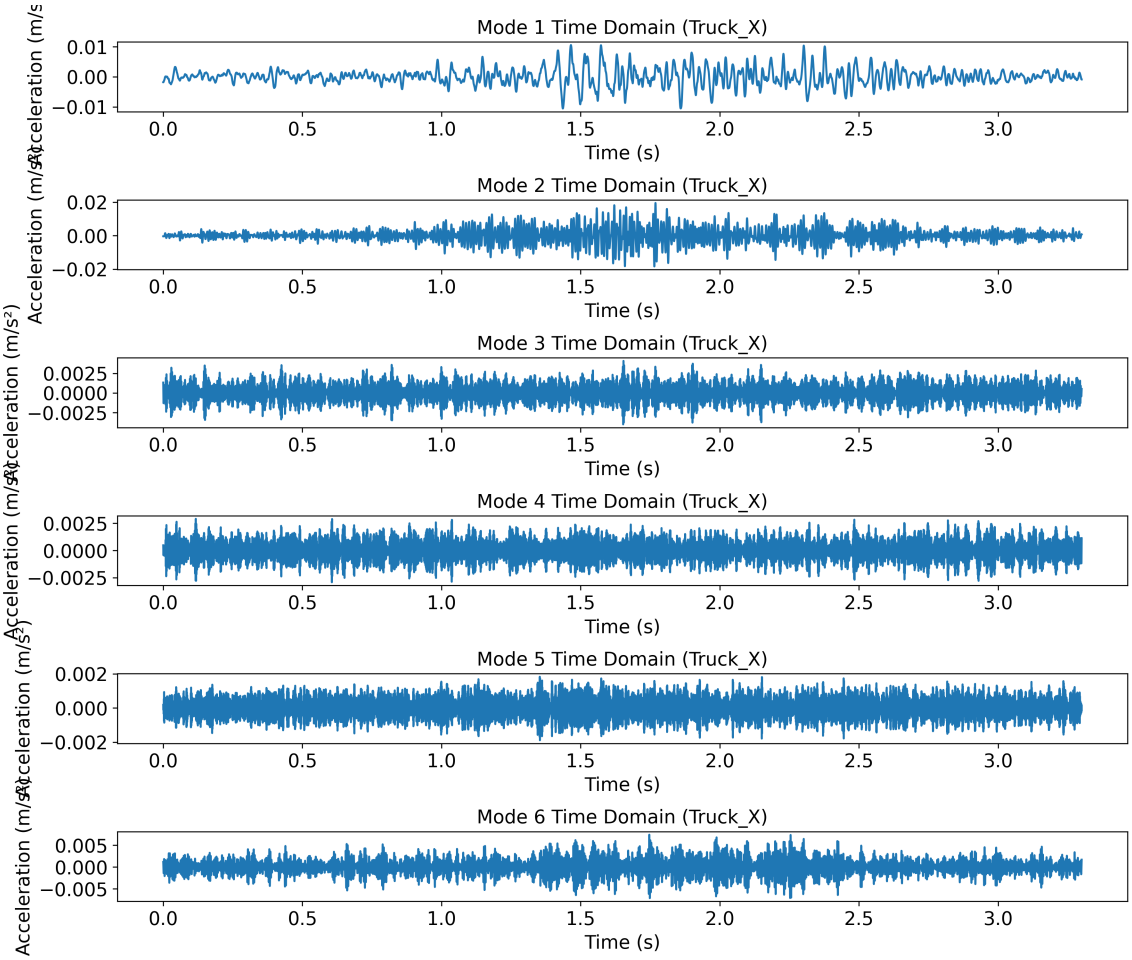

Fig. 5.2 Truck VMD Modes (X direction)

Results for Rumble Strip (X, Y and Z Directions)

This subsection presents the VMD modes of various vehicles on the rumble strip as shown in the Tables 5.2 and 5.3.

Truck: In the X direction, the truck's Mode 1 exhibited moderate vibrations with a maximum value of 0.011 m/s^2 and energy of 0.31 m^2/s^4, dominated by low frequencies (19 Hz). Mode 2 reflected stronger vibrations with higher energy (0.78 m^2/s^4) and frequencies (96 Hz). Beyond Mode 2, the higher modes contribute little, with minimal energy and frequencies extending to 640 Hz by Mode 4. In the Y direction, Mode 1 showed higher maximum values (0.013 m/s^2) and lower frequencies (18 Hz), with Mode 2 following a similar trend but at higher frequencies (104 Hz). Beyond Mode 2, higher modes add minimal vibrational influence. The Z direction revealed the strongest vibrations, with Mode 1 recording 0.021 m/s^2 and high energy (1.10 m^2/s^4), primarily driven by low-frequency vertical displacements (18 Hz). Starting from Mode 3, higher modes contribute progressively less to the vertical dynamics.

Tractor: The tractor in the X direction showed its highest response in Mode 1 with a maximum of 0.023 m/s^2 and energy of 0.66 m^2/s^4, dominated by moderate frequencies (75 Hz). Mode 2 displayed lower energy and higher frequencies (101 Hz). The energy contribution from higher modes beyond Mode 2 diminishes significantly. In the Y direction, Mode 1 recorded a moderate maximum of 0.015 m/s^2, with energy (0.29 m^2/s^4) centered around low frequencies (68 Hz). Mode 2 maintained similar dynamics but shifted to 101 Hz. The higher modes contribute minimally from Mode 3 onwards. In the Z direction, Mode 1 remained dominant with maximum vibrations of 0.019 m/s^2 and energy of 0.37 m^2/s^4, driven by low-frequency components (25 Hz). Beyond Mode 2, higher modes contribute progressively less to the vertical response.

Light Commercial Vehicle (LCV): In the X direction, the LCV's Mode 1 exhibited a significant maximum of 0.022 m/s^2 with energy of 0.57 m^2/s^4 at 94 Hz. Mode 2 followed with decreased maximums but shifted to higher frequencies (263 Hz). Higher modes, starting from Mode 3, provide a limited vibrational contribution. In the Y direction, Mode 1 recorded lower magnitudes with a maximum value of 0.009 m/s^2 and energy of 0.18

m^2/s^4 at 40 Hz. Higher modes contributed little, with frequencies rising to 130 Hz by Mode 2. Mode 1 produced vertical vibrations in the Z direction with a maximum value of 0.014 m/s^2, dominated by low frequencies (20 Hz). The vertical response weakened beyond Mode 2, where frequencies rose and energy diminished.

Car: In the X direction, the car's vibrational response in Mode 1 showed a maximum of 0.005 m/s^2 with low energy (0.03 m^2/s^4) at 29 Hz. Mode 2 shifted to higher frequencies (166 Hz) but exhibited less significant energy (0.02 m^2/s^4). Modes beyond Mode 3 showed minimal contribution. In the Y direction, Mode 1 recorded a maximum value of 0.004 m/s^2 at 61 Hz, with Mode 2 shifting to higher frequencies (135 Hz) but with reduced energy. Beyond Mode 3, the vibrational contribution becomes insignificant. The Z direction followed a similar pattern, with Mode 1 showing a maximum of 0.004 m/s^2 and low energy (0.03 m^2/s^4) at 33 Hz. Higher modes, beyond Mode 3, contributed little.

2-Wheeler: In the X direction, the 2-Wheeler exhibited the strongest vibrational response, with Mode 1 showing a maximum value of 0.036 m/s^2 and energy of 0.62 m^2/s^4 at 26 Hz. Mode 2 showed higher energy (1.52 m^2/s^4) and shifted to higher frequencies (93 Hz). Modes beyond Mode 3 are less significant, contributing little to the overall vibration. In the Y direction, Mode 1 presented a maximum of 0.028 m/s^2 with energy of 0.75 m^2/s^4, also dominated by low frequencies (26 Hz). Mode 2 followed with higher frequencies (93 Hz) and increased energy. Modes beyond Mode 3 contributed minimally. The Z direction displayed the highest vertical response, with Mode 1 producing a maximum value of 0.048 m/s^2 and energy of 1.95 m^2/s^4 at 24 Hz. Mode 2 reflected higher frequencies (107 Hz) but lower energy, while higher modes beyond Mode 3 contributed minimally.

Bus: In the X direction, the bus showed a moderate response in Mode 1 with a maximum value of 0.005 m/s^2 and energy of 0.06 m^2/s^4, dominated by frequencies at 55 Hz. Mode 2 exhibited higher energy (0.08 m^2/s^4) and frequency (119 Hz). The higher modes contributed little to the overall vibration, with frequencies extending to 1020 Hz in

Mode 6. In the Y direction, Mode 1 displayed a maximum of 0.004 m/s^2 and energy of 0.05 m^2/s^4 at 17 Hz. Mode 2 was followed by an increase in both energy and frequency (124 Hz), but higher modes beyond Mode 3 contributed less significantly. The Z direction produced a similar response, with Mode 1 showing a maximum of 0.007 m/s^2 and energy of 0.10 m^2/s^4 at 28 Hz. Mode 2 shifted to higher frequencies (126 Hz) but with decreasing energy. Higher modes beyond Mode 3 contributed minimally to the overall vibrational response.

In rumble strips, the lower modes, particularly Mode 1 and Mode 2, capture the most significant vibration behavior across all vehicles and directions on rumble strips. Beyond Mode 3, higher modes exhibit progressively lower energy and vibration magnitudes, contributing little to the overall dynamic response.

Table 5.2 VMD Mode Features of Rumble Strip (Part 1)

Feature	Mean	Var	Std Dev	RMS	Skew	Kurt	P-P	Max	Min	Cr	Ener	Sh E	MME	DF FFT	DF PSD	SNR
LCV X M1	1.9E-05	1.3E-05	0.004	0.004	-0.102	5.9	0.045	0.022	-0.024	6.5	0.57	5.6	0.024	94	88	1.4
LCV X M2	2.1E-06	4.3E-06	0.002	0.002	0.006	4.2	0.025	0.013	-0.012	6.0	0.18	2.0	0.013	263	263	-6.3
LCV X M3	6.9E-07	8.1E-07	0.001	0.001	-0.001	-0.1	0.007	0.003	-0.003	3.6	0.03	0.5	0.003	430	438	-14.7
LCV Y M1	1.2E-05	4.3E-06	0.002	0.002	0.011	1.6	0.018	0.009	-0.009	4.4	0.18	2.0	0.009	40	50	-4.3
LCV Y M2	2.6E-06	5.2E-06	0.002	0.002	-0.015	3.1	0.025	0.013	-0.012	5.7	0.22	2.4	0.013	130	125	-2.9
LCV Y M3	5.8E-07	1.6E-06	0.001	0.001	-0.005	0.7	0.011	0.006	-0.006	4.7	0.07	0.8	0.006	250	263	-10.0
LCV Z M1	1.0E-05	7.7E-06	0.003	0.003	0.321	2.8	0.025	0.014	-0.011	5.1	0.33	3.4	0.015	20	25	-2.4
LCV Z M2	5.6E-07	3.4E-06	0.002	0.002	0.010	3.7	0.024	0.011	-0.013	6.9	0.14	1.6	0.016	131	125	-6.9
LCV Z M3	8.9E-08	1.3E-06	0.001	0.001	0.006	0.3	0.012	0.006	-0.006	5.4	0.06	0.7	0.006	348	350	-11.8
Bus X M1	2.0E-05	1.9E-06	0.001	0.001	0.062	0.0	0.009	0.005	-0.004	3.4	0.06	0.7	0.005	55	50	-6.5
Bus X M2	3.4E-06	2.8E-06	0.002	0.002	-0.009	1.0	0.014	0.007	-0.007	4.2	0.08	1.0	0.007	119	125	-4.1
Bus X M3	6.9E-07	1.6E-06	0.001	0.001	0.004	0.0	0.009	0.005	-0.005	3.7	0.05	0.6	0.005	273	275	-7.6
Bus Y M1	1.5E-05	1.6E-06	0.001	0.001	-0.228	0.0	0.009	0.004	-0.004	3.5	0.05	0.6	0.005	17	25	-7.6
Bus Y M2	1.7E-06	3.8E-06	0.002	0.002	0.028	1.8	0.018	0.009	-0.009	4.7	0.11	1.3	0.009	124	125	-2.5
Bus Y M3	3.5E-07	1.3E-06	0.001	0.001	0.000	0.0	0.009	0.005	-0.005	4.0	0.04	0.5	0.005	264	263	-8.6
Bus Z M1	1.7E-05	3.4E-06	0.002	0.002	0.199	-0.2	0.012	0.007	-0.005	3.7	0.10	1.2	0.007	28	25	-3.8
Bus Z M2	9.5E-07	2.0E-06	0.001	0.001	0.018	0.6	0.011	0.005	-0.005	3.9	0.06	0.7	0.006	126	125	-6.7
Bus Z M3	2.9E-07	1.7E-06	0.001	0.001	-0.005	-0.2	0.010	0.005	-0.005	4.0	0.05	0.6	0.005	242	238	-7.4
2-W X M1	5.3E-05	2.1E-05	0.005	0.005	0.190	19.5	0.066	0.036	-0.030	7.8	0.62	5.3	0.039	26	25	-4.7
2-W X M2	5.6E-06	5.2E-05	0.007	0.007	0.002	8.6	0.091	0.047	-0.044	6.6	1.52	12.2	0.048	93	88	2.2
2-W X M3	3.4E-07	1.5E-06	0.001	0.001	0.006	0.1	0.009	0.005	-0.005	3.8	0.05	0.6	0.005	344	363	-17.7
2-W Y M1	6.5E-05	2.5E-05	0.005	0.005	0.234	6.8	0.052	0.028	-0.024	5.6	0.75	6.6	0.030	26	25	-5.0
2-W Y M2	6.0E-06	6.0E-05	0.008	0.008	0.024	8.2	0.090	0.046	-0.044	5.9	1.76	14.0	0.046	93	88	1.8
2-W Y M3	4.5E-07	1.6E-06	0.001	0.001	0.001	1.2	0.016	0.007	-0.008	6.5	0.05	0.6	0.008	355	338	-18.3
2-W Z M1	2.5E-05	6.6E-05	0.008	0.008	-0.338	13.1	0.107	0.048	-0.059	7.3	1.95	15.0	0.061	24	25	3.9
2-W Z M2	1.7E-06	7.1E-06	0.003	0.003	-0.071	5.8	0.031	0.015	-0.016	6.0	0.21	2.2	0.017	107	100	-10.8
2-W Z M3	1.5E-07	1.8E-06	0.001	0.001	-0.007	0.5	0.012	0.006	-0.006	4.6	0.05	0.7	0.006	341	350	-17.2

Table 5.3 VMD Mode Features of Rumble Strip (Part 2)

Feature	Mean	Var	Std Dev	RMS	Skew	Kurt	P-P	Max	Min	Cr	Ener	Sh E	MME	DF FFT	DF PSD	SNR
Tru X M1	1.8E-05	7.3E-06	0.003	0.003	0.115	2.0	0.021	0.011	-0.011	3.9	0.31	3.3	0.012	19	25	-5.7
Tru X M2	1.8E-06	1.8E-05	0.004	0.004	0.001	1.6	0.038	0.019	-0.018	4.5	0.78	7.7	0.020	96	100	1.0
Tru X M3	1.2E-07	1.1E-06	0.001	0.001	-0.007	-0.1	0.008	0.004	-0.004	3.9	0.05	0.6	0.004	411	413	-15.2
Tru Y M1	2.2E-05	6.0E-06	0.002	0.002	-0.118	2.4	0.024	0.013	-0.011	5.4	0.25	2.8	0.014	18	25	-5.1
Tru Y M2	2.1E-06	1.2E-05	0.003	0.003	0.013	1.4	0.029	0.016	-0.013	4.6	0.49	5.1	0.016	104	100	-0.2
Tru Y M3	5.5E-07	1.6E-06	0.001	0.001	-0.011	0.2	0.010	0.005	-0.005	4.0	0.07	0.9	0.005	215	213	-11.8
Tru Z M1	3.6E-05	2.6E-05	0.005	0.005	0.179	2.4	0.040	0.021	-0.019	4.2	1.10	10.3	0.025	18	13	1.7
Tru Z M2	1.1E-06	1.0E-05	0.003	0.003	-0.006	1.5	0.026	0.013	-0.013	4.2	0.42	4.4	0.013	145	150	-5.2
Tru Z M3	1.5E-07	1.2E-06	0.001	0.001	-0.003	0.1	0.009	0.004	-0.004	4.0	0.05	0.7	0.005	367	388	-15.5
Tra X M1	4.1E-05	4.0E-05	0.006	0.006	-0.003	1.1	0.049	0.023	-0.026	4.1	0.66	6.1	0.026	75	75	3.5
Tra X M2	1.7E-05	9.6E-06	0.003	0.003	0.038	0.1	0.021	0.011	-0.010	3.5	0.16	1.7	0.011	101	113	-7.0
Tra X M3	1.9E-07	4.5E-07	0.001	0.001	0.000	0.0	0.005	0.002	-0.002	3.7	0.01	0.1	0.002	1077	1075	-21.8
Tra Y M1	3.3E-05	1.7E-05	0.004	0.004	0.006	0.8	0.031	0.015	-0.016	3.9	0.29	2.9	0.016	68	75	1.1
Tra Y M2	1.2E-05	8.0E-06	0.003	0.003	-0.055	-0.1	0.018	0.009	-0.009	3.2	0.13	1.5	0.010	101	100	-4.5
Tra Y M3	1.8E-06	1.4E-06	0.001	0.001	-0.013	0.0	0.009	0.004	-0.005	3.9	0.02	0.3	0.005	278	275	-13.9
Tra Z M1	3.6E-05	2.2E-05	0.005	0.005	-0.011	1.0	0.037	0.019	-0.017	4.1	0.37	3.6	0.020	25	50	-0.4
Tra Z M2	3.1E-06	1.4E-05	0.004	0.004	0.007	0.1	0.024	0.012	-0.012	3.2	0.23	2.4	0.012	169	175	-3.4
Tra Z M3	4.8E-07	1.7E-06	0.001	0.001	-0.004	-0.2	0.009	0.005	-0.005	3.7	0.03	0.3	0.005	418	413	-14.6
Car X M1	4.9E-05	2.1E-06	0.001	0.001	-0.144	0.2	0.010	0.005	-0.005	3.7	0.03	0.4	0.006	29	25	-5.2
Car X M2	6.3E-06	1.2E-06	0.001	0.001	-0.031	0.0	0.008	0.004	-0.004	3.5	0.02	0.3	0.004	166	163	-7.8
Car X M3	2.0E-06	1.3E-06	0.001	0.001	0.005	0.0	0.008	0.004	-0.004	3.7	0.02	0.3	0.004	272	275	-7.7
Car Y M1	3.4E-05	2.3E-06	0.002	0.002	-0.024	-0.4	0.009	0.004	-0.005	3.1	0.04	0.5	0.008	61	63	-4.7
Car Y M2	4.7E-06	1.2E-06	0.001	0.001	-0.033	-0.2	0.007	0.004	-0.004	3.5	0.02	0.3	0.004	135	163	-8.0
Car Y M3	1.6E-06	1.3E-06	0.001	0.001	-0.005	-0.4	0.007	0.004	-0.004	3.2	0.02	0.3	0.004	253	263	-7.8
Car Z M1	8.1E-05	2.0E-06	0.001	0.001	0.122	-0.6	0.007	0.004	-0.003	2.7	0.03	0.4	0.005	33	25	-5.3
Car Z M2	4.5E-06	1.4E-06	0.001	0.001	-0.024	-0.1	0.008	0.004	-0.004	3.3	0.02	0.3	0.006	146	150	-6.9
Car Z M3	1.5E-06	1.2E-06	0.001	0.001	0.002	-0.2	0.007	0.003	-0.004	3.2	0.02	0.3	0.004	275	275	-7.7

Results for Fiber Speed breaker (X, Y and Z Directions)

This subsection presents the VMD modes of various vehicles on the rumble strip as shown in the Table 5.4.

2-Wheeler: In the X direction, the 2-wheeler's Mode 1 exhibited moderate vibrations with a maximum value of 0.013 m/s^2 and energy of 0.44 m^2/s^4, dominated by frequencies at 42 Hz. Mode 2 showed a decrease in maximum value and energy (0.11 m^2/s^4) but a significant shift to higher frequencies (194 Hz). The higher modes beyond Mode 2 showed reduced contributions with minimal energy and high frequencies, such as 712 Hz by Mode 4. In the Y direction, Mode 1 displayed stronger vibrations with a maximum value of 0.024 m/s^2 and energy of 0.43 m^2/s^4, dominated by low-frequency components at 68 Hz. Mode 2 followed with lower energy and higher frequencies (195 Hz). Beyond Mode 2, the higher modes add progressively lower contributions to the overall vibration, with frequencies reaching 892 Hz by Mode 5. In the Z direction, Mode 1 showed moderate vertical vibrations with a maximum value of 0.010 m/s^2 and energy of 0.14 m^2/s^4, dominated by frequencies at 28 Hz. Mode 2 reflected stronger energy (0.16 m^2/s^4) and a shift to higher frequencies (137 Hz). Higher modes beyond Mode 2 contributed less to the vertical response.

Car: In the X direction, the car's Mode 1 showed strong vibrations with a maximum of 0.056 m/s^2 and energy of 3.98 m^2/s^4, dominated by frequencies at 41 Hz. Mode 2 displayed much lower energy (0.23 m^2/s^4) and higher frequencies (71 Hz). Beyond Mode 3, the higher modes contributed minimally to the overall vibration, with frequencies reaching 978 Hz by Mode 5. In the Y direction, Mode 1 produced even stronger vibrations with a maximum of 0.058 m/s^2 and energy of 4.25 m^2/s^4, dominated by frequencies at 41 Hz. Starting from Mode 2, higher modes contributed progressively less energy while shifting to higher frequencies (160 Hz). Beyond Mode 2, the higher modes provide little vibrational influence. In the Z direction, the car's vertical vibrations were strongest in Mode 1, with a

maximum value of 0.030 m/s^2 and energy of 0.92 m^2/s^4, dominated by lower frequencies at 25 Hz. Mode 2 followed with similar dynamics but at higher frequencies (121 Hz). The contribution of higher modes was limited, with frequencies exceeding 765 Hz by Mode 4.

Light Commercial Vehicle (LCV): In the X direction, the LCV's Mode 1 exhibited significant vibrational strength with a maximum value of 0.112 m/s^2 and energy of 5.99 m^2/s^4 at 38 Hz. Mode 2 reflected a shift to higher frequencies (70 Hz) but with reduced energy (3.14 m^2/s^4). Higher modes beyond Mode 3 contributed minimally to the overall vibration, with frequencies extending to 906 Hz in Mode 6. In the Y direction, Mode 1 exhibited strong vibrations with a maximum value of 0.068 m/s^2 and energy of 4.44 m^2/s^4, dominated by frequencies at 38 Hz. Mode 2 showed a shift to higher frequencies (71 Hz) but with lower energy (1.26 m^2/s^4). Beyond Mode 3, the higher modes contributed less, with frequencies reaching 1057 Hz by Mode 5. In the Z direction, Mode 1 produced the highest vertical response, with a maximum value of 0.076 m/s^2 and energy of 2.06 m^2/s^4, driven by lower frequencies (26 Hz). Higher modes, beyond Mode 2, showed limited vibrational influence, with frequencies increasing to 973 Hz by Mode 5.

In fiber breakers, the VMD analysis of the fiber speed breaker shows that lower modes, especially Mode 1 and Mode 2, capture the most significant vibration behavior across all vehicles and directions. Higher modes contribute progressively less energy and vibration magnitudes, with frequencies extending up to 1000 Hz. This analysis highlights the importance of lower modes for understanding the critical vibrational characteristics of fiber speed breakers.

Table 5.4 VMD Mode Features of Fiber Speed Breaker

Feature	Mean	Var	Std Dev	RMS	Skew	Kurt	P-P	Max	Min	Cr	Ener	Sh E	MME	DF FFT	DF PSD	SNR
2-W X M1	8.91E-06	5.51E-06	0.0023	0.0023	-0.35	8.41	0.033	0.013	-0.020	8.5	0.44	4.7	0.020	42	38	-0.4
2-W X M2	6.20E-07	1.37E-06	0.0012	0.0012	0.001	-0.05	0.008	0.004	-0.004	3.6	0.11	1.4	0.004	194	188	-8.6
2-W X M3	2.00E-07	1.25E-06	0.0011	0.0011	-0.003	-0.06	0.008	0.004	-0.004	3.7	0.10	1.3	0.005	306	338	-9.1
2-W Y M1	6.68E-06	5.38E-06	0.0023	0.0023	0.33	12.38	0.043	0.024	-0.018	10.5	0.43	4.6	0.025	68	63	-0.4
2-W Y M2	6.24E-07	1.26E-06	0.0011	0.0011	0.002	-0.03	0.009	0.005	-0.004	4.2	0.10	1.3	0.005	195	188	-8.9
2-W Y M3	2.07E-07	1.14E-06	0.0011	0.0011	0.001	0.06	0.008	0.004	-0.004	3.7	0.09	1.2	0.004	338	325	-9.4
2-W Z M1	9.11E-06	1.74E-06	0.0013	0.0013	0.40	3.63	0.017	0.010	-0.007	7.9	0.14	1.7	0.011	28	38	-6.0
2-W Z M2	8.74E-07	1.99E-06	0.0014	0.0014	0.021	1.33	0.014	0.007	-0.007	5.1	0.16	2.0	0.007	137	125	-5.0
2-W Z M3	2.12E-07	1.24E-06	0.0011	0.0011	0.004	0.09	0.010	0.005	-0.005	4.6	0.10	1.3	0.005	273	275	-7.6
Car X M1	2.14E-05	2.53E-05	0.0050	0.0050	0.56	35.85	0.112	0.056	-0.056	11.2	3.98	31.2	0.060	41	38	5.5
Car X M2	2.74E-06	1.49E-06	0.0012	0.0012	0.10	2.25	0.018	0.010	-0.008	7.8	0.23	2.9	0.010	71	75	-13.1
Car X M3	5.47E-07	1.35E-06	0.0012	0.0012	-0.002	0.00	0.009	0.004	-0.005	3.9	0.21	2.7	0.005	247	275	-13.8
Car Y M1	9.34E-06	2.70E-05	0.0052	0.0052	-0.57	46.87	0.134	0.058	-0.075	14.5	4.25	32.6	0.078	41	38	6.2
Car Y M2	1.05E-06	1.22E-06	0.0011	0.0011	0.003	0.11	0.009	0.005	-0.005	4.3	0.19	2.5	0.008	160	138	-14.2
Car Y M3	2.96E-07	1.18E-06	0.0011	0.0011	0.002	0.05	0.009	0.004	-0.005	4.3	0.19	2.4	0.005	252	263	-14.6
Car Z M1	2.88E-06	5.85E-06	0.0024	0.0024	-2.27	69.88	0.073	0.030	-0.042	17.5	0.92	8.5	0.043	25	25	-2.6
Car Z M2	2.42E-07	5.30E-06	0.0023	0.0023	-0.09	21.81	0.057	0.026	-0.031	13.7	0.84	8.6	0.031	121	125	-3.1
Car Z M3	5.78E-08	1.15E-06	0.0011	0.0011	-0.002	0.02	0.009	0.005	-0.005	4.4	0.18	2.3	0.005	260	250	-11.3
LCV X M1	8.97E-06	5.03E-05	0.0071	0.0071	0.201	78.13	0.210	0.112	-0.098	15.8	5.99	39.8	0.113	38	38	1.8
LCV X M2	2.12E-06	2.63E-05	0.0051	0.0051	0.043	18.95	0.102	0.051	-0.050	10.0	3.14	25.9	0.052	70	75	-3.4
LCV X M3	1.99E-07	1.54E-06	0.0012	0.0012	0.003	0.30	0.013	0.007	-0.006	5.5	0.18	2.3	0.007	248	225	-17.5
LCV Y M1	6.48E-06	3.73E-05	0.0061	0.0061	0.024	29.89	0.136	0.068	-0.069	11.2	4.44	34.0	0.074	38	38	3.5
LCV Y M2	3.17E-06	1.06E-05	0.0033	0.0033	0.197	18.85	0.063	0.033	-0.030	10.1	1.26	11.7	0.034	71	75	-6.1
LCV Y M3	3.29E-07	1.37E-06	0.0012	0.0012	-0.006	0.09	0.010	0.005	-0.005	4.3	0.16	2.1	0.005	241	225	-17.4
LCV Z M1	5.48E-06	1.73E-05	0.0042	0.0042	2.253	106.04	0.135	0.076	-0.059	18.3	2.06	15.5	0.079	26	25	-0.9
LCV Z M2	3.76E-07	1.41E-05	0.0038	0.0038	0.054	23.04	0.084	0.046	-0.039	12.2	1.68	14.9	0.046	124	125	-2.2
LCV Z M3	4.59E-08	1.06E-06	0.0010	0.0010	0.002	0.12	0.010	0.005	-0.005	4.7	0.13	1.6	0.005	333	338	-15.7

Results for Bitumen Speed breaker (X, Y and Z Directions)

This subsection presents the VMD modes of various vehicles on the bituminous speed breaker as shown in the Table 5.5.

Car: In the X direction, the car's Mode 1 exhibited moderate vibrations with a maximum value of 0.03 m/s^2 and energy of 1.76 m^2/s^4, dominated by frequencies at 65 Hz. Mode 2 followed with a decrease in energy (0.12 m^2/s^4) and an increase in dominant frequency (173 Hz). Higher modes beyond Mode 3 contributed progressively less to the overall vibration, with Mode 5 reaching frequencies up to 1074 Hz, indicating minimal vibration. In the Y direction, Mode 1 had a maximum value of 0.02 m/s^2 and energy of 1.36 m^2/s^4, dominated by a frequency of 64 Hz. Beyond Mode 1, subsequent modes showed a decrease in energy and a shift toward higher frequencies. Mode 5 displayed a frequency of 756 Hz but low energy, signifying minimal contribution to the total vibrational response. In the Z direction, the vertical vibrations were strongest in Mode 2, with a maximum value of 0.02 m/s^2 and energy of 0.38 m^2/s^4, dominated by a frequency of 173 Hz. Higher modes beyond Mode 3 contributed minimally, with frequencies reaching 1022 Hz by Mode 5.

2-Wheeler: In the X direction, the 2-wheeler's Mode 1 showed significant vibrations, with a maximum value of 0.02 m/s^2 and energy of 0.91 m^2/s^4, dominated by frequencies at 82 Hz. Mode 2 exhibited a higher crest factor but lower energy (0.10 m^2/s^4) at a frequency of 154 Hz. Beyond Mode 3, the higher modes showed progressively lower contributions, with frequencies extending to 849 Hz by Mode 5. In the Y direction, Mode 1 exhibited the highest vibrational energy with a maximum of 0.02 m/s^2 and energy of 0.85 m^2/s^4, dominated by 82 Hz. Mode 2 displayed lower energy and higher frequencies, while higher modes contributed less to the vibration, with frequencies reaching 961.6 Hz by Mode 5. In the Z direction, the strongest vertical vibrations were observed in Mode 2, with a maximum value of 0.03 m/s^2 and energy of 0.26 m^2/s^4, dominated by a frequency of 126 Hz. The

higher modes showed reduced energy and higher frequencies, with Mode 5 reaching 782 Hz, indicating minimal contribution.

Light Commercial Vehicle (LCV): In the X direction, the LCV's Mode 1 exhibited strong vibrational energy, with a maximum value of 0.07 m/s^2 and energy of 3.05 m^2/s^4, dominated by frequencies at 78 Hz. Mode 2 followed with reduced energy (0.13 m^2/s^4) and higher frequencies at 180 Hz. Beyond Mode 3, the higher modes contributed progressively less to the overall vibration, with frequencies reaching 915 Hz by Mode 5. In the Y direction, Mode 1 exhibited strong vibrations, with a maximum value of 0.03 m/s^2 and energy of 2.21 m^2/s^4, dominated by frequencies at 68 Hz. Beyond Mode 1, higher modes showed progressively lower contributions, with Mode 5 reaching a 961 Hz frequency but with minimal energy. In the Z direction, Mode 1 showed moderate vertical vibrations, with a maximum value of 0.02 m/s^2 and energy of 0.48 m^2/s^4, dominated by frequencies at 28 Hz. Mode 2 followed with increased crest factor and energy (0.27 m^2/s^4), dominated by 143 Hz. Higher modes beyond Mode 3 contributed minimally to the vertical vibration response, with frequencies extending to 961 Hz by Mode 5.

The VMD analysis of the bitumen speed breaker indicates that the first two modes, especially Mode 1 and Mode 2, capture the most significant vibration characteristics across all vehicles and directions. Higher modes beyond Mode 3 contribute minimally, with frequencies extending up to 1000 Hz. This analysis shows that lower modes are the key to understanding the primary vibrational responses on bitumen speed breakers.

Table 5.5 VMD Mode Features of Bitumin Speed Breaker

Feature	Mean	Var	Std Dev	RMS	Skew	Kurt	P-P	Max	Min	Cr	Ener	Sh E	MME	DF FFT	DF PSD	SNR
Car X M1	8E-06	3E-05	5E-03	5E-03	-0.03	3.36	0.053	0.027	-0.027	5.3	1.76	16.4	0.027	66	75	6
Car X M2	1E-06	2E-06	1E-03	1E-03	0.01	1.29	0.013	0.006	-0.007	5.1	0.12	1.5	0.007	174	175	-12
Car X M3	4E-07	1E-06	1E-03	1E-03	-0.01	-0.04	0.009	0.004	-0.005	4.2	0.08	1.1	0.005	292	288	-14
Car Y M1	1E-05	2E-05	4E-03	4E-03	0.03	1.44	0.038	0.018	-0.020	4.5	1.36	13.3	0.020	65	63	5
Car Y M2	2E-06	1E-06	1E-03	1E-03	-0.05	1.87	0.016	0.007	-0.008	7.0	0.09	1.2	0.009	112	125	-13
Car Y M3	6E-07	1E-06	1E-03	1E-03	0.0028	-0.16	0.008	0.004	-0.004	4.0	0.07	1.0	0.004	276	275	-14
Car Z M1	1E-05	5E-06	2E-03	2E-03	-0.13	0.81	0.019	0.011	-0.008	5.3	0.32	3.6	0.012	51	38	-4
Car Z M2	9E-07	6E-06	2E-03	2E-03	-0.01	8.23	0.038	0.018	-0.019	8.2	0.38	4.0	0.019	174	175	-2
Car Z M3	3E-07	1E-06	1E-03	1E-03	-0.001	-0.03	0.008	0.004	-0.004	3.9	0.08	1.1	0.004	287	288	-11
2-W X M1	2E-05	2E-05	4E-03	4E-03	-0.19	6.64	0.058	0.024	-0.034	8.4	0.91	8.7	0.034	82	75	4
2-W X M2	4E-06	2E-06	1E-03	1E-03	-0.18	9.66	0.027	0.014	-0.013	10.4	0.10	1.2	0.014	154	150	-11
2-W X M3	1E-06	1E-06	1E-03	1E-03	0.0031	-0.22	0.008	0.004	-0.004	3.8	0.07	0.9	0.004	298	300	-13
2-W Y M1	1E-05	2E-05	4E-03	4E-03	-0.06	2.53	0.039	0.019	-0.020	5.1	0.85	8.4	0.022	83	75	4
2-W Y M2	2E-06	1E-06	1E-03	1E-03	-0.04	0.82	0.015	0.008	-0.007	6.7	0.08	1.0	0.008	171	175	-11
2-W Y M3	8E-07	1E-06	1E-03	1E-03	-0.0039	-0.02	0.009	0.004	-0.004	3.8	0.07	0.9	0.004	310	313	-12
2-W Z M1	3E-05	3E-06	2E-03	2E-03	0.11	1.32	0.018	0.010	-0.007	6.1	0.15	1.8	0.010	23	25	-6
2-W Z M2	2E-06	5E-06	2E-03	2E-03	-0.015	38.74	0.059	0.029	-0.029	13.6	0.26	2.6	0.031	126	125	-2
2-W Z M3	7E-07	1E-06	1E-03	1E-03	0.0066	2.01	0.018	0.009	-0.009	8.3	0.07	0.9	0.009	255	250	-10
LCV X M1	7E-06	4E-05	6E-03	6E-03	-0.36	28.47	0.139	0.068	-0.071	11.6	3.05	24.4	0.073	79	75	8
LCV X M2	1E-06	2E-06	1E-03	1E-03	0.06	6.53	0.029	0.015	-0.014	12.0	0.13	1.6	0.016	181	175	-14
LCV X M3	4E-07	1E-06	1E-03	1E-03	0.0036	-0.11	0.009	0.005	-0.004	4.5	0.10	1.3	0.005	293	288	-16
LCV Y M1	2E-05	3E-05	5E-03	5E-03	-0.0351	6.67	0.075	0.034	-0.042	8.0	2.21	20.1	0.042	68	75	7
LCV Y M2	2E-06	1E-06	1E-03	1E-03	-0.0202	0.28	0.012	0.005	-0.007	6.1	0.11	1.4	0.007	168	188	-14
LCV Y M3	7E-07	1E-06	1E-03	1E-03	-0.0032	0.04	0.009	0.004	-0.004	3.9	0.10	1.3	0.005	297	300	-14
LCV Z M1	9E-06	6E-06	2E-03	2E-03	0.0947	4.83	0.032	0.015	-0.016	6.8	0.48	5.2	0.017	28	38	-2
LCV Z M2	6E-07	3E-06	2E-03	2E-03	0.2385	22.50	0.052	0.029	-0.022	16.0	0.27	3.0	0.029	143	150	-5
LCV Z M3	2E-07	1E-06	1E-03	1E-03	0.0019	0.02	0.011	0.005	-0.005	4.8	0.10	1.3	0.006	297	300	-10

5.3 Discussion

5.3.1 Impact of Vehicle Type and Breaker Profiles on Vibration Metrics

The study's data reveal distinct vibration profiles generated by each vehicle type across varied speed breaker designs, specifically when examining peak acceleration, RMS and total energy across the X, Y and Z axes.

Vehicle Weight and Axle Distribution: Heavier vehicles exert a greater force on speed breakers, translating into higher peak accelerations and RMS values. For instance, on rumble strips, the truck's peak lateral acceleration in X direction reached 0.0444 m/s^2 as shown in Figure 5.1, in contrast to 0.0291 m/s^2 for cars in Figure 5.1. This elevated value aligns with the increased axle load in trucks, which amplifies downward force when crossing segmented obstacles like rumble strips. Lighter vehicles, like cars, show lower acceleration max values and total energy values in the X direction than heavier vehicles due to a lower load distribution per axle. These differences are particularly apparent on fiber speed breakers, where the material's rigidity amplifies the impact for heavier vehicles. LCVs recorded 0.1159 m/s^2 maximum acceleration and 4.078 m^2/s^4 in total energy in X direction on fiber speed breakers as shown in Figure 5.1, higher than the 0.0291 m/s^2 maximum acceleration observed for cars on rumble strips. This discrepancy underscores the sensitivity of fiber speed breakers to axle load.

Suspension System Response: Each vehicle's suspension response also influences vibrational energy transfer, with trucks and buses typically having stiffer suspensions. This characteristic supports higher loads and amplifies vibration when encountering rigid speed breakers like fiber or rumble strips. For instance, the total energy recorded for the bus on the bitumen speed breaker was 42.91 m^2/s^4 for X direction (Figure 5.1), significantly surpassing values for lighter vehicles, which reflects the dampening limitations of stiffer

suspensions in absorbing vibrations generated by abrupt geometries. Lighter vehicles, such as cars and 2-wheelers, have suspension systems generally tuned for smoother road interaction, resulting in lower energy values even on rigid speed breakers. For example, the car recorded a maximum acceleration in the X direction of 0.0418 m/s^2 on the fiber speed breaker (Figure 5.1), a much lower value than heavier vehicles like LCVs.

Breaker Geometry and Material Properties: The smoother, larger radius of bitumen speed breakers minimizes abrupt impacts, reflected in lower peak vertical accelerations in the Z direction and total energy values for various vehicle types. For example, the max acceleration in the Z direction for the LCV on the bitumen speed breaker was 0.0122 m/s^2 (Figure 5.1), lower than that observed on fiber or rumble strips. Fiber and rumble strips, with their rigid, discontinuous surfaces, generate higher-frequency responses and pronounced peak values, particularly in vertical and lateral directions. The rigid composition of fiber speed breakers produces higher frequencies and more sudden jolts. For instance, the dominating frequency for the LCV in the Z-axis was 200 Hz on rumble strips (Figure 5.1, a stark contrast to the 70 Hz dominating frequency on the smoother fiber speed breaker. These variations align with each speed breaker type's distinct material responses and vehicle impacts.

5.3.2 Directional Vibration Characteristics

Each directional component (X, Y, Z) responds uniquely to the speed breaker type and vehicle characteristics, revealing insights into how road obstacles influence structural dynamics.

Lateral (X-axis) Vibrations: Lateral vibrations, indicated by RMS in X direction values (m/s^2), show heightened responses on narrower, more rigid speed breakers like fiber speed breakers, which induce a swaying effect, especially in vehicles with a higher center of gravity, such as trucks and buses. For instance, the fiber speed breaker induced an RMS

in X direction of 0.0178 m/s^2 in the LCV, compared to 0.0045 m/s^2 on the bitumen speed breaker (Figure 5.1). This pronounced increase could be attributed to tilting as vehicles traverse the narrow, raised fiber speed breaker profile, causing significant lateral motion.

Longitudinal (Y-axis) Vibrations: Longitudinal vibrations (Y-axis) generally display moderate maximum and RMS values on smoother speed breakers, such as bitumen, where the gradual transition reduces abrupt longitudinal impacts. The RMS in the Y direction for the bus (Figure 5.1 on the bitumen speed breaker was 0.0430 m/s^2, aligning with the relatively smooth engagement along the speed breaker's length, which minimizes abrupt accelerations. Conversely, the rumble strip produces higher frequencies and accelerations longitudinally. For instance, a truck (Figure 5.1 recorded 0.0372 m/s^2 for max acceleration in the Y direction on rumble strips due to the frequent, abrupt interaction with the speed breaker's segmented surface, which disturbs the vehicle's forward momentum.

Vertical (Z-axis) Vibrations: Vertical vibrations, representing the Z direction, reveal how speed breaker stiffness and geometry significantly influence the vibrational response, with higher max acceleration in Z direction values (m/s^2) recorded on more protruding and rigid speed breakers. Due to its simpler suspension, the tractor (Figure 5.1 displayed heightened Z-axis vibrations on bitumen compared to fiber. It had a max acceleration in the Z direction of 0.0488 m/s^2 and a dominating frequency at 178 Hz. This indicates a more direct transfer of vertical forces in vehicles with less dampening capability, as the energy is not absorbed effectively by the suspension, leading to higher frequencies in the vertical domain. Similarly, with their stiff composition, fiber speed breakers recorded elevated vertical response values due to their immediate contact force during passage.

5.3.3 VMD-Based Signal Decomposition

This study provides a comprehensive analysis of vehicle vibrations induced by different types of speed breakers, such as bitumen speed breakers, fiber speed breakers and rumble

strips, using Variational Mode Decomposition (VMD). The extracted mode features from the vibration signals, as presented in Tables 5.5, 5.4, 5.2 and 5.3, offer valuable insights into the vibrational behavior of various vehicle types, including two-wheelers (2-W), three-wheelers (3-W), cars, light commercial vehicles (LCVs), trucks (Tru) and tractors (Tra). The VMD modes are depicted with mode numbers as M1, M2, etc. Additionally, the dimensions of the speed breakers, characterized by height, width and the height-to-width (H/W) ratio, play a crucial role in influencing the vibration responses.

Influence of Speed Breaker Design and Dimensions on Vibration Characteristics

The design and dimensions of speed breakers significantly influence the vibrational responses of vehicles by altering the amplitude and frequency content of the induced vibrations. The height, width and H/W ratio determine the profile and steepness of the speed breakers, affecting how vehicles interact with them.

Bitumen Speed Breakers exhibit a gradual elevation with a greater width and lower H/W ratio, resulting in a gentler incline. This design leads to smoother vehicle transitions, allowing the suspension systems to absorb vibrations more effectively. Both lighter and heavier vehicles exhibit significant energy in the initial modes (Modes 1 and 2) when traversing bitumen speed breakers, but with lower skewness and kurtosis values. This indicates more Gaussian-like vibration characteristics, reflecting smoother and less abrupt impacts. For example, in Table 5.5, mode 1 of the LCV in x direction LCV X M1 has an energy of 3.05 in Mode 1. In contrast, mode 1 of the car in the x direction, Car X M1, shows an energy of 1.76, indicating effective vibration absorption by the suspension systems of heavier vehicles.

Fiber Speed Breakers, characterized by a higher H/W ratio due to their steeper incline and narrower width, induce more abrupt impacts, leading to higher vibration amplitudes and energies, particularly in lighter vehicles with less effective damping. The data indicates elevated skewness and kurtosis values in the initial modes for lighter vehicles, signifying

impulsive forces and non-Gaussian vibration characteristics. For instance, in Table 5.4, the mode 1 of the car in the x direction, Car X M1, exhibits an energy of 3.98 in Mode 1 with a kurtosis of 35.85, reflecting the presence of impulsive vibrations caused by the steep and narrow profile of fiber speed breakers.

Rumble Strips, consisting of multiple narrow strips with a moderate H/W ratio, introduce repeated impacts due to their segmented design. This results in increased oscillatory responses and higher-frequency vibrations. The cumulative effect of traversing six strips leads to elevated energy in higher modes (Modes 3 and above), especially for lighter vehicles. For example, in Table 5.3, the mode 3 of the car in the x direction, Car X M3, exhibits an energy of 0.02 in Mode3, indicating susceptibility to high-frequency vibrations induced by the repeated impacts of rumble strips.

Influence of Vehicle Type on Vibration Responses

The vehicle type plays a crucial role in the vibrational response due to mass, suspension stiffness and structural design differences.

Lighter Vehicles (Two-Wheelers, Three-Wheelers and Cars) exhibit significant energy in the initial modes across all types of speed breakers. Still, the impact is more pronounced with fiber speed breakers and rumble strips. Higher skewness and kurtosis values in the initial modes indicate impulsive and non-Gaussian vibration characteristics. This is attributed to lighter vehicle's lower mass and stiffer suspensions, which are less effective at damping high-frequency vibrations induced by abrupt changes in road profiles. For example, mode 3 of the 2-wheeler in x direction 2-W X M3 in Table 5.4 has an energy of 0.10 with dominant frequencies of 306Hz (FFT) and 338Hz (PSD), highlighting the susceptibility of two-wheelers to high-frequency excitations.

Heavier Vehicles (LCVs, Trucks and Tractors) also show significant energy in the initial modes, but with lower skewness and kurtosis values, indicating smoother and more Gaussian-like vibration characteristics. The higher mass and more compliant suspensions

of heavier vehicles effectively dampen vibrations, even when traversing speed breakers with higher H/W ratios. For instance, the mode 1 of the Tractor in z direction Tra Z M1 in Table 5.3 has an energy of 0.37 with dominant frequencies of 25Hz (FFT) and 50Hz (PSD), reflecting effective vibration absorption by the suspension systems.

Directional Vibrations and Vehicle Component Responses

Analyzing vibrations along different axes provides insights into the contributions of various vehicle components and the impact on vehicle dynamics.

Vertical (Z-Axis) vibrations are significantly influenced by the height and H/W ratio of the speed breakers. Steeper speed breakers induce higher vertical accelerations. Lighter and heavier vehicles exhibit significant energy in the initial modes along the Z-axis. However, lighter vehicles show higher skewness and kurtosis, indicating that their suspensions are less effective at absorbing vertical impacts, leading to discomfort and potential mechanical stress.

Longitudinal (X-Axis) vibrations are affected by the width of the speed breakers and the presence of multiple strips in rumble strips. Narrow and steep speed breakers and repeated impacts from rumble strips lead to rapid, successive impacts that can influence the drivetrain and chassis. Lighter vehicles exhibit elevated energy and higher dominant frequencies in the initial modes along the X-axis, indicating potential impacts on acceleration, braking forces and drivetrain components. For example, mode 3 of the 2-wheeler in x direction 2-W X M3 in Table 5.4 has dominant frequencies of 306Hz (FFT) and 338Hz (PSD), reflecting the influence of drivetrain dynamics.

Lateral (Y-Axis) vibrations, although generally less pronounced, are crucial for assessing vehicle stability and handling. Elevated RMS and energy values in the Y-axis modes suggest significant lateral vibrations affecting steering response and passenger comfort, particularly in lighter vehicles traversing narrow speed breakers like fiber speed breakers.

Dominant Frequencies and Energy Distribution Across Modes

The dominant frequencies and energy distribution across modes provide further insights into vehicle responses and potential resonance phenomena.

Initial Modes (Modes 1 and 2) capture the fundamental vibration characteristics for all vehicle types. The dominant frequencies in these modes are generally in the lower range (20- 50Hz), corresponding to the natural frequencies of the suspension system and vehicle body modes. For heavier vehicles, the energy concentration in Modes 1 and 2 indicates effective damping and absorption of vibrations by the suspension systems. For example, the mode of the tractor in z direction, mode 1 of the tractor in z direction, Tra Z M1 in Table 5.3 has dominant frequencies of 25Hz (FFT) and 50Hz (PSD), with significant energy content.

Higher Modes (Modes3 and Above) capture higher-frequency vibrations, which are more pronounced in lighter vehicles. These modes are associated with unsprung mass dynamics, tire enveloping frequencies and chassis resonances. The elevated energy in these modes for cars and two-wheelers indicates susceptibility to high-frequency vibrations induced by rigid speed breakers and rumble strips. For instance, mode 3 of the car in the x direction, Car X M3 in Table 5.3, exhibits dominant frequencies of 272Hz (FFT) and 275Hz (PSD), reflecting excitation of higher-order structural modes.

Statistical Features Indicating Vibration Characteristics

Statistical measures such as skewness and kurtosis provide insights into the vibration's nature and potential impact.

- **High Skewness and Kurtosis**: Elevated skewness and kurtosis values in the initial modes, especially for lighter vehicles traversing fiber speed breakers and rumble strips, indicate impulsive and non-Gaussian vibration characteristics. For example, the mode 1 of the car in x direction Car X M1 in Table 5.4 has a skewness of 0.56 and kurtosis of 35.85, suggesting sharp peaks and heavy tails in the vibration signal distribution. This reflects transient shocks that are less effectively absorbed by

the suspension system, potentially leading to discomfort and increased mechanical stress.

- **Low Skewness and Kurtosis**: Lower skewness and kurtosis values in heavier vehicles suggest more symmetrical and Gaussian-like vibration distributions, implying effective vibration absorption. For instance, the mode 1 of the LCV in z direction LCV Z M1 in Table 5.5 exhibits a skewness of 0.0947 and kurtosis of 4.83, indicating smoother vibration profiles conducive to structural integrity and passenger comfort.

Mode Energy and Dominant Frequency Patterns

The significant energy concentration in the initial modes across all vehicle types highlights the fundamental importance of these modes in capturing the primary vibration response.

- **Mode1**: Captures the fundamental vibrations corresponding to the suspension system and vehicle body motions. For example, the mode 1 of the LCV in x direction LCV X M1 in Table 5.4 has an energy of 5.99, indicating a substantial amount of vibration energy is absorbed in this mode.

- **Higher Modes**: Capture higher-frequency vibrations related to structural resonances, tire dynamics and drivetrain vibrations. Elevated energy and dominant frequencies in these modes, such as in the mode 3 of the car in x direction Car X M3 and mode 3 of the 2-wheeler in x direction 2-W X M3 in Table 5.4, indicate potential resonance with specific vehicle components, leading to increased noise, vibration and harshness (NVH) levels.

Implications for Vehicle Design and Road Engineering

The findings have several practical and impactful implications:

1. *Vehicle Suspension Optimization*: Manufacturers can optimize suspension systems based on vehicle class and operating environment. For lighter vehicles frequently

traversing speed breakers with higher H/W ratios, suspensions can be engineered to absorb high-frequency vibrations better. This may involve using advanced damping materials, tuned mass dampers, or active suspension technologies to enhance ride comfort and reduce mechanical stress.

2. *Speed Breaker Design Optimization*: Road engineers can design speed breakers that achieve desired speed control while minimizing adverse vibrations. Implementing speed breakers with lower H/W ratios and greater widths, as seen with bitumen speed breakers, can reduce abrupt impacts. This design approach allows smoother transitions, enabling vehicle suspensions to absorb vibrations more effectively and enhancing safety and comfort for all vehicle types.

3. *Infrastructure Planning and Policy*: Understanding the interaction between vehicle types and speed breaker dimensions can inform infrastructure planning. Policies can encourage standardizing speed breaker designs based on traffic composition and vehicle dynamics. In areas with high volumes of lighter vehicles, avoiding steep and narrow speed breakers can enhance safety and comfort. Additionally, promoting the adoption of advanced suspension systems in lighter vehicles can further mitigate vibration issues.

Enhancing Safety and Comfort

Aligning speed breaker designs with vehicle vibration characteristics can lead to significant improvements in safety and comfort:

- *For Drivers and Passengers*: Reducing exposure to uncomfortable and potentially harmful vibrations enhances the driving experience, reduces fatigue and improves safety by maintaining driver alertness and control. Prolonged exposure to high-frequency vibrations can lead to health issues such as lower back pain and musculoskeletal disorders.

- *For Vehicles*: Minimizing harmful vibrations extends the lifespan of components, particularly in lighter vehicles where high-frequency vibrations can cause fatigue failures in structural elements and electronic systems. This contributes to lower maintenance costs and increased reliability.

- *For Road Infrastructure*: Appropriate speed breaker designs reduce dynamic loads on road surfaces, lowering maintenance requirements and preventing premature pavement deterioration. This has economic benefits in terms of reduced repair costs and extended infrastructure lifespan.

Scientific Explanation of Observed Patterns

The observed patterns can be scientifically explained based on vehicle dynamics and vibration theory:

- *Mass-Spring-Damper Systems*: Vehicles can be modeled as mass-spring-damper systems, where the mass represents the vehicle body, the spring represents the suspension stiffness and the damper represents the shock absorber. Heavier vehicles have larger masses and often more compliant suspensions, resulting in lower natural frequencies and effective damping of higher-frequency vibrations. Lighter vehicles, with lower mass and stiffer suspensions, have higher natural frequencies and less effective damping, making them more susceptible to high-frequency excitations.

- *Resonance Phenomena*: When the excitation frequency matches the natural frequency of a vehicle component, resonance occurs, leading to amplified vibrations. With their repeated impacts at regular intervals, Rumble strips can induce resonance in vehicle components, particularly in lighter vehicles. This explains the elevated energy observed in higher modes and the increased discomfort experienced by occupants.

- *Impulse-Momentum Relationship*: The abrupt changes in road profile associated with speed breakers with higher H/W ratios result in sudden changes in momentum, leading to higher impulsive forces. These forces manifest as sharp peaks in the vibration signals, indicated by high kurtosis values and are less effectively absorbed by the suspensions of lighter vehicles.

- *Fourier Transform Analysis*: The dominant frequencies identified through FFT and PSD correspond to the frequencies with the highest energy content in the vibration signals. The distribution of these frequencies across modes reflects the vehicle's response to the speed breaker profiles and the efficiency of the suspension system in attenuating different frequency components.

- *Statistical Signal Characteristics*: Skewness and kurtosis provide information about the symmetry and peakedness of the vibration signal distribution. High kurtosis indicates the presence of outliers or extreme values, often associated with impulsive forces. These statistical measures help understand the non-linear and transient nature of the vibrations experienced by different vehicles.

The VMD-based analysis offers a comprehensive and scientifically robust understanding of vehicle vibrations induced by different speed breaker designs and dimensions. By identifying dominant frequencies, energy distributions and statistical characteristics, this study provides valuable insights that can inform vehicle design improvements, predictive maintenance strategies and optimized road engineering practices.

The findings emphasize the importance of considering vehicle characteristics and speed breaker dimensions to enhance safety, efficiency and comfort in transportation systems. Future research could explore developing advanced suspension systems capable of adapting to varying road profiles and implementing innovative road technologies that dynamically adjust to traffic conditions.

5.4 Conclusion

This study presents a detailed multi-directional (X, Y, Z) vibration analysis of three speed hump types, namely Fiber, Bitumen and Rumble Strips, across a wide range of vehicles, including two-wheelers, three-wheelers, cars, LCVs, trucks, tractors and buses. Using a hybrid experimental and analytical approach, vibration data were collected via tri-axial accelerometers and processed with advanced signal decomposition through Variational Mode Decomposition (VMD). Results reveal significant variations in vibration amplitudes, total energy and frequency components due to differences in hump design, vehicle mass distribution and suspension systems.

From a technical perspective, Fiber and Rumble Strip humps consistently induce higher vibration amplitudes and energy, especially affecting lighter vehicles with limited damping. Their vibration signatures often show impulsive, non-Gaussian traits with elevated skewness and kurtosis. In contrast, Bitumen humps distribute impact forces more uniformly, yielding lower acceleration peaks and smoother frequency profiles. The VMD analysis shows lower-mode predominance, where the first two modes capture most vibration energy, indicating that geometric and material adjustments at these resonant bands can effectively mitigate adverse effects.

Directional analyses reveal stronger vertical (Z-axis) and longitudinal (X-axis) accelerations on narrower, more abrupt profiles, reflecting the pronounced jolt when vehicles navigate steep inclines or segmented surfaces. Vehicles with stiffer suspensions, such as heavier trucks and buses, manage to dampen part of the high-frequency loads but still register significantly elevated amplitudes on rigid humps. Conversely, lighter vehicles like two or three-wheelers encounter more severe high-frequency components, especially over discontinuous surfaces like Rumble Strips. These findings indicate that adequate material choice, hump geometry and speed management can better align with varying suspension designs.

Practically, these insights support refining speed hump design. In areas needing strict speed control, rigid profiles (Fiber, Rumble Strips) deter speeding but raise vibrations, suggesting the need for advanced suspension or subgrade modifications. On busy corridors where comfort and structural life matter, smoother Bitumen humps or added damping layers can reduce harmonic excitations and wear. Additionally, using gentler hump inclines for heavy vehicles may lessen excessive vertical loads, minimizing pavement damage and driver discomfort.

The VMD-based frequency decomposition enhances conventional time-domain analysis by identifying critical resonant zones in each vehicle-hump interaction. It distinguishes low-frequency components tied to chassis motion and higher-frequency modes linked to tire, axle, or body resonances. This frequency-specific insight, combined with amplitude features (peak, RMS, energy), supports more nuanced, data-driven mitigation strategies, including refined suspension tuning or hump geometries tailored to local traffic.

Looking ahead, future investigations may extend to hybrid or electric vehicles with distinct weight and suspension profiles, further broadening the scope of hump design optimization. Integrating real-time measurement systems (e.g., distributed fiber optics) and machine learning models could refine predictive analyses, enabling dynamic adjustments or adaptive hump solutions in smart transportation networks. This study lays a solid foundation for bridging safety-oriented speed control with minimized vibrational impacts, advancing resilient, comfortable and efficient urban infrastructure.

While the findings in this chapter highlight the amplifying effects of geometric discontinuities such as speed humps on vehicular vibration patterns, the subsequent chapter focuses on vibrations recorded over smooth, uninterrupted pavements. This shift enables the formulation of standardized vibration indices, free from geometric artifacts and forms the foundation for comparative vibration quantification across vehicle classes.